

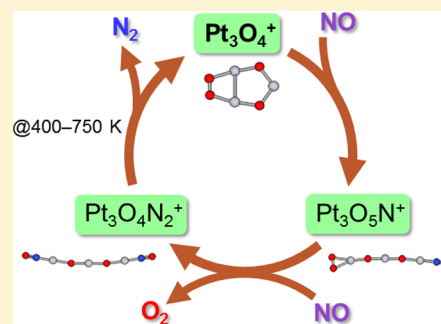
Catalytic Decomposition of NO by Cationic Platinum Oxide Cluster Pt_3O_4^+

Jun Yamagishi, Ken Miyajima, Satoshi Kudoh, and Fumitaka Mafuné*

Department of Basic Science, School of Arts and Sciences, The University of Tokyo, Komaba, Meguro, Tokyo 153-8902, Japan

S Supporting Information

ABSTRACT: The catalytic decomposition of NO by cationic platinum oxide cluster Pt_3O_4^+ was investigated by mass spectrometry and thermal desorption spectrometry. Upon reaction with two NO molecules, molecular oxygen desorbed from the cluster at room temperature to form $\text{Pt}_3\text{O}_4\text{N}_2^+$. Then, at temperatures above 400 K, desorption of N_2 from $\text{Pt}_3\text{O}_4\text{N}_2^+$ was observed. These processes were confirmed by isotope-labeling experiments, and the energetics of O_2 and N_2 release were determined by density functional calculations. The combination of these elementary steps resulted in the catalytic decomposition of NO by Pt_3O_4^+ .



Platinum is widely used as a catalyst in a variety of chemical reactions in industrial processes. The development of new efficient catalytic systems is necessary to understand the catalytic properties of Pt-based catalysts. Platinum is an important component of three-way catalysts^{1,2} and plays a role as a hydrocarbon oxidation enhancer^{3,4} and in the reduction of nitrogen oxides to N_2 .⁵ Catalytic NO decomposition, reduction, and oxidation reactions are a challenging task,^{6–11} and the selectivity of Pt catalysts toward N_2 or N_2O is known to be affected by the support material, Pt dispersion, and temperature.^{10,12} Thus, it is crucial to understand the interactions and reaction mechanisms between nitrogen oxides, platinum metal, and platinum oxides. In this study, we examined the behavior of platinum oxide species formed in the presence of oxygen.

Metal clusters have been widely used as model catalytic systems, and their reaction mechanism with different gases has been extensively investigated.^{13–16} In particular, several experimental^{17–21} and theoretical studies^{22–25} on the reactivity of Pt clusters have been reported. Balaj et al. have determined the rate constants for the reaction of Pt clusters with N_2O ^{17–19} and, more recently, we reported the oxygen transfer reaction between neutral Pt clusters and N_2O .²⁶ The reaction rates and number of steps exhibit a strong and irregular dependence on the cluster size and its charge state. Hermes et al. observed the infrared-activated CO oxidation reaction by infrared multiphoton dissociation spectroscopy of $\text{Pt}_n\text{O}_m\text{CO}^+$.²⁷ Recently, Crampton et al. investigated the catalytic ethylene hydrogenation reaction on size-selected Pt_n ($n = 8–15$) clusters soft-landed on magnesia.²⁸

In this study, the reaction between NO and platinum oxide clusters was investigated by a combination of mass spectrometry (MS) and thermal desorption spectroscopy (TDS), and the experimental findings were compared with density functional theory (DFT) calculations.

At first, platinum oxide clusters were prepared and characterized by TDS. The mass spectra of the platinum oxide cluster cations Pt_nO_m^+ ($n = 1–4$, $m = 0–7$) obtained when the O_2 concentration in the He carrier gas was 0.5% were recorded and are shown in Figure S1. At room temperature, platinum oxide clusters with $(n, m) = (1, [0, 3–4, 6])$, $(2, 3–5)$, $(3, 3–7)$, and $(4, 4–7)$ were observed, in which the number of O atoms was equal to or greater than that of Pt atoms ($n \leq m$). The temperature dependence of the intensity ratio of platinum oxide cluster cations Pt_3O_m^+ was measured (Figure 1), and Pt_3O_4^+ was found to be the most abundant cluster over the whole temperature range. In the temperature range of 300–500 K, an increase of the cluster with $m = 4$ and a concomitant decrease of that with $m = 6$ was observed, indicating the release of molecular oxygen from Pt_3O_6^+ .

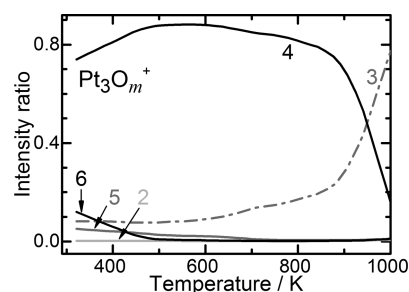


Figure 1. Temperature dependence of the intensity ratio of Pt_3O_m^+ ($m = 2–6$) produced in the presence of 0.5% O_2 diluted in He as the carrier gas.

Received: March 10, 2017

Accepted: April 26, 2017

Published: April 26, 2017



Notably, the less oxygenated cluster cation Pt_3O_2^+ , which was expected to be formed by continuous oxygen desorption, was not observed even at 800 K, clearly demonstrating the thermal durability of Pt_3O_4^+ cluster. This agrees well with the facts that the decomposition of $\alpha\text{-PtO}_x$ ($x \sim 1.4$) in an O_2 ambient is accompanied by formation of crystalline Pt_3O_4 phase formed before reaching metallic Pt,²⁹ and bulk Pt_3O_4 is thermodynamically stable in a region around 900 K at atmospheric pressure.³⁰

Next, the reaction of Pt_3O_4^+ with NO was performed by introducing He-diluted NO gas through the pulsed gas valve, and the NO concentration dependence of the intensity ratio of $\text{Pt}_3\text{O}_m\text{N}_k^+$ at room temperature was measured, as shown in Figure 2.

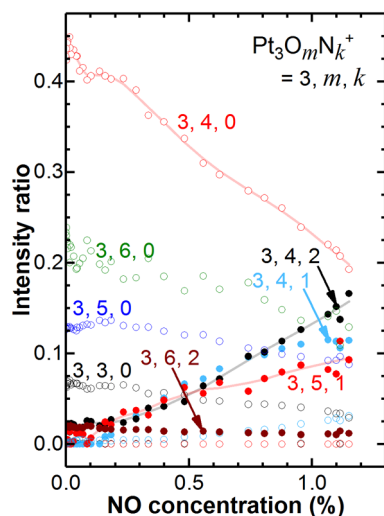


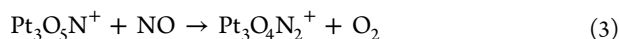
Figure 2. Intensity ratio of $\text{Pt}_3\text{O}_m\text{N}_k^+$ as a function of the NO concentration in the reaction gas at room temperature.

The intensity of Pt_3O_4^+ monotonically decreased with increasing NO concentration. Although present in small quantities, the intensity of other platinum oxide clusters, namely, Pt_3O_3^+ , Pt_3O_5^+ , and Pt_3O_6^+ , also decreased.

On the other hand, the intensities of $\text{Pt}_3\text{O}_5\text{N}^+$, $\text{Pt}_3\text{O}_4\text{N}^+$, and $\text{Pt}_3\text{O}_4\text{N}_2^+$ clusters increased. $\text{Pt}_3\text{O}_5\text{N}^+$ is a simple NO adduct formed by the following reaction:



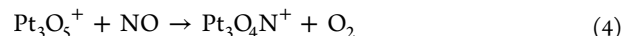
However, because Pt_3O_2^+ was not present under these conditions, $\text{Pt}_3\text{O}_4\text{N}_2^+$ could not be formed in the same manner. It was noted that the increase of $\text{Pt}_3\text{O}_5\text{N}^+$ was about half of the decrease of parent Pt_3O_4^+ , and the decrease of parent Pt_3O_4^+ corresponded to the total increase of reaction products $\text{Pt}_3\text{O}_5\text{N}^+$ and $\text{Pt}_3\text{O}_4\text{N}_2^+$. In addition, the secondary NO adduct $\text{Pt}_3\text{O}_6\text{N}_2^+$ (formed by the reaction of Pt_3O_4^+ with 2NO) was not observed, suggesting that NO addition and O_2 desorption proceeded simultaneously. Thus, the following O_2 desorption reaction was envisioned:



As discussed later, this reaction scheme was supported by isotope-labeling experiments and DFT calculations.

Because of the NO concentration dependence of $\text{Pt}_3\text{O}_4\text{N}^+$, this cluster appeared to derive from the combination of Pt_3O_3^+

and NO. However, the increase of $\text{Pt}_3\text{O}_4\text{N}^+$ was not balanced by the decrease of Pt_3O_3^+ . Thus, besides the simple NO addition to Pt_3O_3^+ , the following reaction was assumed to occur:



This reaction scheme is supported by the fact that, with increasing NO concentration, the decrease of Pt_3O_5^+ did not correspond to the formation of $\text{Pt}_3\text{O}_6\text{N}^+$. Thus, the common reaction pathway in which Pt oxide clusters react with NO and release O_2 at room temperature was envisioned.

Moreover, the thermal desorption spectra of $\text{Pt}_3\text{O}_m\text{N}_k^+$ ($m = 0-6$) measured at a NO concentration of 0.8% (Figure 3)

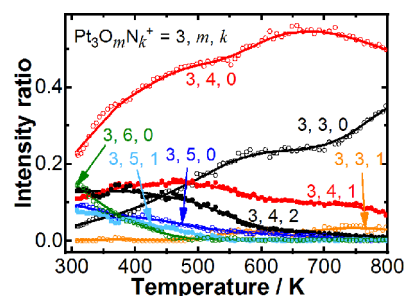


Figure 3. Thermal desorption spectra of $\text{Pt}_3\text{O}_m\text{N}_k^+$ at a NO concentration of 0.8%.

confirmed that the O_2 release from Pt_3O_6^+ (reaction in eq 1) proceeded in the temperature range of 300–500 K, as seen in Figure 1. The other clusters, namely, $\text{Pt}_3\text{O}_4\text{N}_2^+$, $\text{Pt}_3\text{O}_5\text{N}^+$, $\text{Pt}_3\text{O}_4\text{N}^+$, and $\text{Pt}_3\text{O}_3\text{N}^+$, formed by reaction with NO, showed temperature dependence.

In the case of $\text{Pt}_3\text{O}_5\text{N}^+$, NO release occurred in the temperature range of 300–550 K:

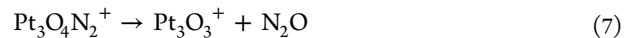


On the other hand, for $\text{Pt}_3\text{O}_4\text{N}_2^+$, N_2 desorption was observed in the temperature range of 400–750 K:



In contrast, $\text{Pt}_3\text{O}_4\text{N}^+$, containing one less nitrogen atom, remained almost intact at temperatures up to 700 K. These results show that some platinum oxide clusters have the ability to decompose NO at room temperature.

It should be noted that the gradual increase of Pt_3O_3^+ in the low-temperature region (300–600 K) was significant compared to that observed in Figure 1, presumably because of the following reactions:



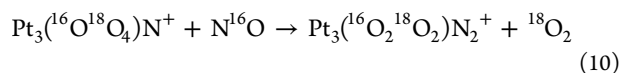
The $\text{Pt}_3\text{O}_3\text{N}^+$ increase at high temperatures (500–800 K) might be attributed to NO release:



Next, the origin of the oxygen atoms in the platinum oxide clusters was investigated by preparing the clusters using a He-diluted $^{18}\text{O}_2$ gas and determining the change in ^{18}O content after the N^{16}O reaction. The mass spectra of isotope-labeled $\text{Pt}_3^{18}\text{O}_{3,4}^+$ ions with thermal desorption at 700 K were measured before and after the N^{16}O reaction (Figure S2)

using a $N^{16}O$ concentration of 0.06%. Before the introduction of $N^{16}O$, $Pt_3^{18}O_3^+$ and $Pt_3^{18}O_4^+$ were abundantly observed. For $Pt_3O_3^+$, ^{16}O isotope contamination was detected; for instance, $Pt_3(^{16}O_1^{18}O_2)^+$ and $Pt_3(^{16}O_1^{18}O_3)^+$ species were found. It is likely that clusters containing an even number of oxygen atoms were formed by the sequential addition of $^{18}O_2$ to bare platinum clusters, whereas clusters containing an odd number of oxygen atoms originated from the laser ablation of surface oxide layer ($Pt^{16}O_x$).

After the reaction with $N^{16}O$, the peak intensities of $Pt_3(^{16}O_2^{18}O_2)N^+$, $Pt_3(^{16}O^{18}O_3)N^+$, and $Pt_3(^{16}O_2^{18}O_2)N_2^+$ increased. Whereas $Pt_3(^{16}O_2^{18}O_2)N^+$ and $Pt_3(^{16}O^{18}O_3)N^+$ derived from the NO addition to $Pt_3(^{16}O^{18}O_2)^+$ and $Pt_3^{18}O_3^+$, respectively, $Pt_3(^{16}O_2^{18}O_2)N_2^+$ was not a simple NO adduct because $Pt_3^{18}O_2^+$ was not present in the system. Thus, the reaction in eq 3 can be expressed in more detail as follows:



This result shows that the molecular oxygen desorbed at room temperature originated from the platinum oxide core and not from the reactant NO gas. As expected, no peaks due to simple NO addition to $Pt_3O_4^+$ were observed because $Pt_3O_5N^+$ decomposed at temperatures >550 K (see eq 5).

The experimental results revealed that O_2 was released upon the reaction of $Pt_3O_4^+$ with two NO molecules. An energy diagram of the NO adsorption reaction on $Pt_3O_4^+$ was constructed in which the most stable structures at each step were determined by DFT calculations (Figure 4). Interestingly,

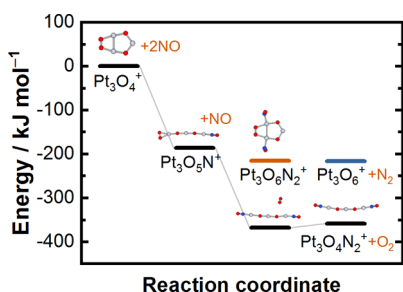


Figure 4. Energy diagram of NO adsorption on $Pt_3O_4^+$. Pt, N, and O atoms are shown in gray, blue, and red, respectively.

the sequential NO addition (eq 2 \rightarrow eq 3) to form $Pt_3O_4N_2^+$ was found to be exothermic. In addition, the energy level of the products derived from O_2 release, i.e., $Pt_3O_4N_2^+$ and O_2 , was lower than the alternative reaction products, i.e., $Pt_3O_6^+$ and N_2 . Thus, the theoretical calculations confirmed our previously described reaction scheme proceeding via O_2 release.

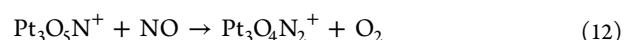
The geometrical structure of the final product after O_2 emission, i.e., $Pt_3O_4N_2^+$, was found to be linear. In addition, NO molecules were added molecularly; in other words, no N–O bond cleavage occurred. We can therefore conclude that the released O_2 molecule derived from the parent platinum oxide cluster $Pt_3O_4^+$, which is in agreement with the results of the isotope-labeling experiment (eq 10).

In summary, the reaction of $Pt_3O_4^+$ with NO proceeded by the following three steps:

First NO addition



Second NO addition accompanied by O_2 release



N_2 release upon heating (400–750 K)



The reaction in eq 13 gives $Pt_3O_4^+$, which is the starting ion in eq 11. Hence, a reaction cycle can be proposed, as shown in the graphic contained in the abstract. Whereas the first and second reactions proceeded at room temperature, the final step required heating at around 400–750 K. This is reasonable, because eq 13 requires the large bending motion of the linear chain in order to produce the most stable isomer of $Pt_3O_4^+$. The isotope-labeling experiment showed that the released O_2 molecule derived from the oxygen atoms of original $Pt_3O_4^+$ and not from the added NO molecules; however, in the subsequent cycles, the O_2 molecule released is composed of the oxygen atoms of previously incorporated NO. The structure of recycled $Pt_3O_4^+$ is supposed to be the most stable ring structure, because the linear isomer of $Pt_3O_4^+$ is 63 kJ mol $^{-1}$ higher in energy. Overall, two NO molecules are decomposed and converted into O_2 and N_2 in the catalytic cycle of $Pt_3O_4^+$.

In conclusion, the reaction of platinum oxide clusters and NO was studied by a combination of mass spectrometry and DFT calculations. At room temperature, the reaction of $Pt_3O_4^+$ with NO resulted in NO addition and O_2 release. Temperature desorption experiments showed N_2 release from $Pt_3O_4N_2^+$, to achieve an overall catalytic cycle. The proposed reaction scheme was supported by the results of DFT calculations and isotope-labeling experiments.

EXPERIMENTAL AND COMPUTATIONAL METHODS

The $Pt_3O_4^+$ -catalyzed decomposition of NO was investigated by TDS and MS. Details of the experimental setup are shown in Figure S3.^{31–33} The gas-phase Pt clusters were formed in a cluster source: a Pt metal rod (Furuya Metal Co., Ltd.) was vaporized by a Nd:YAG pulsed laser (355 nm) in the presence of 0.5% oxygen diluted with helium (total stagnation pressure = 0.8 MPa). The generated $Pt_nO_m^+$ ($n = 1–4$) reacted with NO molecules in the fast flow reactor where He-diluted NO gas was introduced through a gas valve. After the reaction, the clusters were placed in an extension tube, in which the temperature was controlled in the range of 300–1000 K. The residence time of the cluster ions in the tube exceeded 100 μ s, and the number density of helium atoms exceeded 10^{18} cm $^{-3}$. Hence, the clusters underwent more than 10 000 collisions with helium, ensuring that thermal equilibrium was achieved in the tube. Pseudo-TDS plots were obtained by scanning the temperature range.

For the mass analysis, the $Pt_nO_m^+$ clusters expanded into vacuum at the end of the extension tube and gained a kinetic energy of +3.5 keV in the acceleration region. The clusters traveled in a 1 m field-free region, were reversed by a dual-stage reflectron, and were then detected with a Hamamatsu double-microchannel plate detector. The mass resolution was sufficiently high (>1000 at $m/z = 1000$) to distinguish Pt and O isotopic peaks in the mass spectra. For the interpretation of complex mass spectra containing multiple Pt isotopic peaks, a homemade isotope pattern deconvolution program was used.³⁴

To estimate the NO adsorption energy to $Pt_3O_4^+$, we performed DFT calculations using the Gaussian 09 program.³⁵ The LANL2DZ effective core potential and basis set were used to describe the Pt atoms,³⁶ whereas the 6-31G(d) basis set was

used to describe the N and O atoms.³⁷ Becke's three-parameter hybrid density functional³⁸ with the Lee–Yang–Parr correlation functional (B3LYP) were used for all calculations.³⁹

■ ASSOCIATED CONTENT

Supporting Information

The Supporting Information is available free of charge on the ACS Publications website at DOI: 10.1021/acs.jpclett.7b00591.

Mass spectrum of Pt_nO_m^+ ($n = 1-4$) produced in 0.5% oxygen diluted in helium at room temperature (Figure S1), intensity change of isotope-labeled $\text{Pt}_3^{18}\text{O}_{3.4}^+$ ion with thermal desorption at 700 K before and after the N^{16}O reaction (Figure S2), and schematic view of the experimental setup (Figure S3) (PDF)

■ AUTHOR INFORMATION

Corresponding Author

*E-mail: mafune@cluster.c.u-tokyo.ac.jp.

ORCID

Fumitaka Mafuné: 0000-0001-8860-6354

Notes

The authors declare no competing financial interest.

■ ACKNOWLEDGMENTS

This work was supported by a Grant-in-Aid for Scientific Research (A) (No. 25248004) and a Grant-in-Aid for Exploratory Research (No. 26620002) from the Ministry of Education, Culture, Sports, Science and Technology, Japan (MEXT).

■ REFERENCES

- (1) Zhdanov, V. P.; Kasemo, B. Mechanism and Kinetics of the NO–CO Reaction on Rh. *Surf. Sci. Rep.* **1997**, *29* (2), 31–90.
- (2) Di Monte, R.; Kašpar, J. On the Role of Oxygen Storage in Three-Way Catalysis. *Top. Catal.* **2004**, *28* (1–4), 47–57.
- (3) Vendelbo, S. B.; Elkjær, C. F.; Falsig, H.; Puspitasari, I.; Dona, P.; Mele, L.; Morana, B.; Nelissen, B. J.; van Rijn, R.; Creemer, J. F.; et al. Visualization of Oscillatory Behaviour of Pt Nanoparticles Catalysing CO Oxidation. *Nat. Mater.* **2014**, *13*, 884–890.
- (4) Chen, L.; Chen, B.; Zhou, C.; Wu, J.; Forrey, R. C.; Cheng, H. Influence of CO Poisoning on Hydrogen Chemisorption onto a Pt₆ Cluster. *J. Phys. Chem. C* **2008**, *112* (36), 13937–13942.
- (5) Burch, R.; Breen, J. P.; Meunier, F. C. A Review of the Selective Reduction of NO_x with Hydrocarbons under Lean-Burn Conditions with Non-Zeolitic Oxide and Platinum Group Metal Catalysts. *Appl. Catal., B* **2002**, *39* (4), 283–303.
- (6) Mei, D.; Du, J.; Neurock, M. First-Principles-Based Kinetic Monte Carlo Simulation of Nitric Oxide Reduction over Platinum Nanoparticles under Lean-Burn Conditions. *Ind. Eng. Chem. Res.* **2010**, *49* (21), 10364–10373.
- (7) Després, J.; Elsener, M.; Koebel, M.; Kröcher, O.; Schnyder, B.; Wokaun, A. Catalytic Oxidation of Nitrogen Monoxide over Pt/SiO₂. *Appl. Catal., B* **2004**, *50* (2), 73–82.
- (8) Xue, E.; Seshan, K.; Ross, J. R. H. Roles of Supports, Pt Loading and Pt Dispersion in the Oxidation of NO to NO₂ and of SO₂ to SO₃. *Appl. Catal., B* **1996**, *11* (1), 65–79.
- (9) Demicheli, M. C.; Hoang, L. C.; Ménéz, J. C.; Barbier, J.; Pinabiau-Carlier, M. Influence of Metal Particle Size and Effect of Gold Addition on the Activity and Selectivity of Pt/Al₂O₃ Catalysts in the Reduction of Nitric Oxide by Methane. *Appl. Catal., A* **1993**, *97*, L11–L17.
- (10) Lee, J.-H.; Kung, H. H. Effect of Pt Dispersion on the Reduction of NO by Propene over Alumina-Supported Pt Catalysts under Lean-Burn Conditions. *Catal. Lett.* **1998**, *51* (1–2), 1–4.
- (11) Getman, R. B.; Xu, Y.; Schneider, W. F. Thermodynamics of Environment-Dependent Oxygen Chemisorption on Pt(111). *J. Phys. Chem. C* **2008**, *112* (26), 9559–9572.
- (12) Ono, L. K.; Yuan, B.; Heinrich, H.; Cuenya, B. R. Formation and Thermal Stability of Platinum Oxides on Size-Selected Platinum Nanoparticles: Support Effects. *J. Phys. Chem. C* **2010**, *114* (50), 22119–22133.
- (13) Lang, S. M.; Bernhardt, T. M. Gas Phase Metal Cluster Model Systems for Heterogeneous Catalysis. *Phys. Chem. Chem. Phys.* **2012**, *14* (26), 9255–9269.
- (14) Castleman, A. W.; Jena, P. Clusters: A Bridge between Disciplines. *Proc. Natl. Acad. Sci. U. S. A.* **2006**, *103* (28), 10552–10553.
- (15) Johnson, G. E.; Tyo, E. C.; Castleman, A. W. Cluster Reactivity Experiments: Employing Mass Spectrometry to Investigate the Molecular Level Details of Catalytic Oxidation Reactions. *Proc. Natl. Acad. Sci. U. S. A.* **2008**, *105* (47), 18108–18113.
- (16) Böhme, D. K.; Schwarz, H. Gas-Phase Catalysis by Atomic and Cluster Metal Ions: The Ultimate Single-Site Catalysts. *Angew. Chem., Int. Ed.* **2005**, *44* (16), 2336–2354.
- (17) Balteanu, I.; Petru Balaj, O.; Beyer, M. K.; Bondybey, V. E. Reactions of Platinum Clusters $^{195}\text{Pt}_n^+$, $n = 1-24$, with N₂O Studied with Isotopically Enriched Platinum. *Phys. Chem. Chem. Phys.* **2004**, *6* (11), 2910–2913.
- (18) Balaj, O. P.; Balteanu, I.; Roßteuscher, T. T. J.; Beyer, M. K.; Bondybey, V. E. Catalytic Oxidation of CO with N₂O on Gas-Phase Platinum Clusters. *Angew. Chem., Int. Ed.* **2004**, *43* (47), 6519–6522.
- (19) Parry, I. S.; Kartouzian, A.; Hamilton, S. M.; Balaj, O. P.; Beyer, M. K.; Mackenzie, S. R. Collisional Activation of N₂O Decomposition and CO Oxidation Reactions on Isolated Rhodium Clusters. *J. Phys. Chem. A* **2013**, *117* (36), 8855–8863.
- (20) Adlhart, C.; Uggerud, E. Reactions of Platinum Clusters Pt_n^+ , $n = 1-21$, with CH₄: To React or Not to React. *Chem. Commun.* **2006**, No. 24, 2581–2582.
- (21) Koszinowski, K.; Schröder, D.; Schwarz, H. Reactivity of Small Cationic Platinum Clusters. *J. Phys. Chem. A* **2003**, *107* (25), 4999–5006.
- (22) Hintz, P. A.; Ervin, K. M. Chemisorption and Oxidation Reactions of Nickel Group Cluster Anions with N₂, O₂, CO₂, and N₂O. *J. Chem. Phys.* **1995**, *103* (18), 7897–7906.
- (23) Xu, Y.; Shelton, W. A.; Schneider, W. F. Thermodynamic Equilibrium Compositions, Structures, and Reaction Energies of Pt_xO_y ($x = 1-3$) Clusters Predicted from First Principles. *J. Phys. Chem. B* **2006**, *110* (33), 16591–16599.
- (24) Zhang, X.-G.; Armentrout, P. B. Activation of O₂ and CO₂ by PtO⁺: The Thermochemistry of PtO₂⁺. *J. Phys. Chem. A* **2003**, *107* (42), 8915–8922.
- (25) Lv, L.; Wang, Y.; Jin, Y. On the Catalytic Mechanism of Pt₄⁺ in the Oxygen Transport Activation of N₂O by CO. *Theor. Chem. Acc.* **2011**, *130* (1), 15–25.
- (26) Yamamoto, H.; Miyajima, K.; Yasuike, T.; Mafuné, F. Reactions of Neutral Platinum Clusters with N₂O and CO. *J. Phys. Chem. A* **2013**, *117* (47), 12175–12183.
- (27) Hermes, A. C.; Hamilton, S. M.; Cooper, G. A.; Kerpál, C.; Harding, D. J.; Meijer, G.; Fielicke, A.; Mackenzie, S. R. Infrared Driven CO Oxidation Reactions on Isolated Platinum Cluster Oxides, Pt_nO_m⁺. *Faraday Discuss.* **2012**, *157*, 213–225.
- (28) Crampton, A. S.; Rötzer, M. D.; Ridge, C. J.; Schweinberger, F. F.; Heiz, U.; Yoon, B.; Landman, U. Structure Sensitivity in the Non-scalable Regime Explored via Catalysed Ethylene Hydrogenation on Supported Platinum Nanoclusters. *Nat. Commun.* **2016**, *7*, 10389.
- (29) Saenger, K. L.; Cabral, C.; Lavoie, C.; Rossnagel, S. M. Thermal Stability and Oxygen-Loss Characteristics of Pt(O) Films Prepared by Reactive Sputtering. *J. Appl. Phys.* **1999**, *86* (11), 6084–6087.
- (30) Seriani, N.; Pompe, W.; Ciacchi, L. C. Catalytic Oxidation Activity of Pt₃O₄ Surfaces and Thin Films. *J. Phys. Chem. B* **2006**, *110* (30), 14860–14869.

- (31) Mafuné, F.; Takenouchi, M.; Miyajima, K.; Kudoh, S. Rhodium Oxide Cluster Ions Studied by Thermal Desorption Spectrometry. *J. Phys. Chem. A* **2016**, *120* (3), 356–363.
- (32) Miyajima, K.; Mafuné, F. Release of Oxygen from Palladium Oxide Cluster Ions by Heat. *J. Phys. Chem. A* **2015**, *119* (29), 8055–8061.
- (33) Koyama, K.; Kudoh, S.; Miyajima, K.; Mafuné, F. Thermal Desorption Spectroscopy Study of the Adsorption and Reduction of NO by Cobalt Cluster Ions under Thermal Equilibrium Conditions at 300 K. *J. Phys. Chem. A* **2015**, *119* (37), 9573–9580.
- (34) Miyajima, K.; Mafuné, F. Catalytic Reactions of Gas Phase Zirconium Oxide Clusters with NO and CO Revealed by Post Heating. *Chem. Phys. Lett.* **2016**, *660*, 261–265.
- (35) Frisch, M. J.; Trucks, G. W.; Schlegel, H. B.; Scuseria, G. E.; Robb, M. A.; Cheeseman, J. R.; Scalmani, G.; Barone, V.; Mennucci, B.; Petersson, G. A.; Nakatsuji, H.; Caricato, M.; Li, X.; Hratchian, H. P.; Izmaylov, A. F.; Bloino, J.; Zheng, G.; Sonnenb, D. J. *Gaussian 09*; Gaussian, Inc.: Wallingford, CT, 2009.
- (36) Hay, P. J.; Wadt, W. R. Ab Initio Effective Core Potentials for Molecular Calculations. Potentials for K to Au Including the Outermost Core Orbitals. *J. Chem. Phys.* **1985**, *82* (1), 299–310.
- (37) Krishnan, R.; Binkley, J. S.; Seeger, R.; Pople, J. A. Self-Consistent Molecular Orbital Methods. XX. A Basis Set for Correlated Wave Functions. *J. Chem. Phys.* **1980**, *72* (1), 650–654.
- (38) Becke, A. D. Density-Functional Thermochemistry. III. The Role of Exact Exchange. *J. Chem. Phys.* **1993**, *98* (7), 5648–5652.
- (39) Lee, C.; Yang, W.; Parr, R. G. Development of the Colle-Salvetti Correlation-Energy Formula into a Functional of the Electron Density. *Phys. Rev. B: Condens. Matter Mater. Phys.* **1988**, *37* (2), 785–789.